Polypropylene/organoclay/SEBS nanocomposites with toughness–stiffness properties

Catalina-Gabriela Sanporean (née Potarniche),†*[a] Zina Vuluga,†*[b]
Constantin Radovici,[b] Denis Mihaela Panaitescu,[b] Michaela Iorga,[b]
Jesper deClaville Christiansen[a] and Alessandra Mosca[c]

Polypropylene nanocomposites with a different amount of styrene-ethylene-butylene-styrene block copolymer (SEBS)/clay were prepared *via* a melt mixing technique. To improve the dispersion of commercial organoclay (denoted as OMMT), various amounts of SEBS were incorporated. At a fixed content of OMMT, the mechanical properties were improved with increasing SEBS content. The obtained nanocomposites were characterized through X-ray diffraction (XRD), differential scanning calorimetry (DSC-TG) and mechanical tests. The thermal–morphological–mechanical properties were investigated. The nanomaterials presented an improved decomposition temperature, a small decrease in tensile strength, a higher Young's modulus and a spectacular increase of 300% in impact strength.

Introduction

Nanocomposites' structures have opened revolutionary possibilities in the development of new materials. The addition of layered silicates in polymer systems leads to a great improvement in their properties such as thermal stability and mechanical performance. This is because the high surface area of these particles with nanometric dimensions increases the interfacial interactions between the matrix and clay.[1–8]

In order to achieve a nanocomposite with improved properties, different formulations have been tested until now, one of the most used polymer for obtaining nanocomposites is polypropylene (PP). To obtain polypropylene nanocomposites based on layered silicates, a compatibilizer needs to be added, due to the incompatibility between the two components. As compatibilizer, maleated polypropylene (MA-PP)[9–16] and maleated styrene-6-(ethylene-cobutylenes)-6-styrene triblock copolymer (MA-SEBS)[17–21] were used because of the interaction which the maleic group can give with layered silicates. It has been reported that SEBS can also be used as compatibilizer for PP nanocomposites, on one hand due to benzyl groups which interact with the clay platelets[2,22,23] and on the other hand due to the butylene parts which can interact with the PP chain.

The mechanical and processing properties of the SEBS/PP blend have been greatly improved.[24–28] The most used fillers for

PP microcomposites are calcium carbonate, mica, and short glass fiber.[29–31] The properties of fibre reinforced microcomposites containing a rubbery phase such as styrene-ethylene-butylene-styrene (SEBS), ethylene-propylene rubber and ethylene-propylene-diene monomer elastomer were intensively studied.[32,33] Tjong *et al.*[34] study the mechanical properties of glass fibre reinforced PP/SEBS hybrids. They report that the glass fibre reinforced composites toughened with SEBS elastomers exhibit good tensile properties, improved impact strength, and fracture toughness. In general, the structure and mechanical properties of PP composites strongly depend on the interfacial adhesion between the filler and matrix, the dispersion of filler particles, and processing conditions.

In automotive industry new materials are being developed with superior properties in terms of electrical, conductivity and gloss applications and the tendency is to replace the old ones.[35–37] Nowadays, there are currently being used materials which exhibit high stiffness properties, but poor toughness properties like PP/glass fibres composites.[38,39] These types of materials are used to obtain car parts which require high impact properties thus increased toughness too, like the bumper beam.

The incorporation of the filler into PP/elastomer blends can restore the required stiffness and strength, leading to superior properties.[18]

To the authors' best knowledge, few papers are reported in literature[1,23,40,41] on nanocomposite based on PP, SEBS and layered silicate. This research is a continuation of our work published by Z. Vuluga *et al.*[41] in which the authors presented preliminary results on this topic. Most of the studies on this material mainly discuss the interaction between components and present morphological characterisation. Mechanical properties were poorly investigated and on materials which contain

[a]*Department of Mechanical and Manufacturing Engineering, Aalborg University, 9220 Aalborg, Denmark. E-mail: gabi@m-tech.aau.dk*

[b]*National Research and Development Institute for Chemistry and Petrochemistry-ICECHIM, Bucharest, Romania. E-mail: zvuluga@yahoo.com*

[c]*Technical University of Denmark, Center for Elektronnanoskopi, 2800 Kgs Lyngby, Denmark*

† These authors contributed equally.

slightly different systems for example Cloiste 20A as filler with maleated polypropylene as compatibilizing agent. In this study the uses of SEBS had a threefold reason: to increase the toughness of the material, to find the right concentration of SEBS at which the stiffness was not drastically affected and to be used as compatibilizer. However, this material was not intensively studied and needs to have our attention in order to understand the structure–properties relationship.

In this study, nanocomposites based on PP, SEBS and ditallow-dimethyl-ammonium ion modified natural montmorillonite (OMMT) were prepared using extrusion. The organo-modified montmorillonite that was used in this study contained higher amount of ammonium quaternary salt as compared with previous studies in which Cloisite 20A was used. This work studies a broad range of concentrations of OMMT and of SEBS in order to investigate their influence on toughness–stiffness properties and contributes to the improvement of already existent results by correlating thermal–morphological–mechanical properties. The results of the intercalated structure and mechanical properties of PP/OMMT/SEBS nanocomposites were reported and discussed.

Experimental part

Materials

The PP matrix used for this study was a homopolymer produced by LyondellBasell. The grade name is HP400R and has the density = 0.905 g cm^{-3}, a melt flow rate = 25 g per 10 min at 230 °C, 2.16 kg load. An organo-modified clay (Dellite 67G, powder), which is a dimethyl dihydrogenated tallow ammonium ion modified natural montmorillonite (OMMT), was supplied by Laviosa Chimica Mineraria (Livorno, Italy). The block copolymer used was a linear styrene-ethylene-butylene-styrene with 30% polystyrene, M_n = 79 100, MFI = 5.00 g per 10 min (230 °C per 5 kg) (Kraton 1652 G SQR 1000).

Preparation of PP/OMMT/SEBS nanocomposites

The organo-modified clay Dellite 67G was compounded with SEBS using a DSE 20 Brabender Twin Screw Extruder (160 ± 5 °C, 240 rpm). Four types of masterbatches were obtained with different SEBS : OMMT weight ratio 1.2 : 1; 1.4 : 1; 1.6 : 1 and 2 : 1.

The nanocomposites were obtained in dynamical conditions using the same DSE 20 Brabender Twin Screw Extruder, by dispersing previous obtained masterbatches of OMMT modified with block copolymer into a PP matrix. The composition of the obtained nanomaterials is presented in Table 1. The obtained granules were injected into standard bars for mechanical tests.

In order to understand the toughness–stiffness properties and for comparison, polypropylene containing different OMMT concentrations and polypropylene with different SEBS concentrations, were obtained using the same procedure described above.

Characterisation

The basal spacing, d_{001}, was determined by means of X-ray diffraction (XRD) on a DRON diffractometer; the CoKα radiation

Table 1 Composition of PP/SEBS nanocomposites

Sample name	PP (%)	Silicate (%)	SEBS (%)
PP/1/1.2	97.8	1	1.2
PP/2/2.4	96.5	2	2.4
PP/2.5/3.5	94	2.5	3.5
PP/3/3.6	93.4	3	3.6
PP/5/7	88	5	7
PP/10/12	78	10	12
PP/10/14	76	10	14
PP/10/16	74	10	16
PP/10/20	70	10	20

source (λ = 1.79021 Å) was used filtered with Fe for removing Kβ component, in the Bragg–Brentano system (by reflection); the patterns were automatically recorded at small angles (2θ: 1.3 ÷ 12°).

DSC-TG analyses were carried out using a Netzsch DSC-TG type STA 449 C Jupiter differential scanning calorimeter-thermal analyser. About 5 mg of each nanocomposite was weighed in the Al_2O_3 DSC pan and placed in the DSC cell. The samples were heated in the temperature range of 25 °C to 550 °C, at a heating rate of 10 °C min^{-1} and under a current of air of 50 cm^3 min^{-1}. The % of crystalline phase (X) was estimate using the following equation:

$$X = \frac{\Delta H}{w \times \Delta H_{100}} \times 100 \tag{1}$$

where ΔH is the enthalpy of melting for the analysed sample, and ΔH_{100} is the reference value for the enthalpy of melting of 100% crystalline polymer and w is the weight fraction of PP in nanocomposite. For isotactic polypropylene, ΔH_{100} is 209 J g^{-1}.[42]

An FEI Titan T20 TEM microscope operating at 200 kV was used for 2D imaging of nanocomposites.

Tensile, creep and cyclic tests were carried out on a universal tensile machine INSTRON, Norwood, Massachusetts 5586, equipped with a 50 kN load cell and a video extensometer with the gauge length of 50 mm (series 2663-882). Tensile test specimens were obtained on an industrial-sized Ferromatik Milacron, Malterdingen, Germany K110 injection-molding machine according to ISO 3167 multipurpose specimen with the cross-sectional area of 10 mm × 4 mm.

The Izod impact strength was determined according to SR EN ISO 180:2001, using a Ceast pendulum impact tester.

The Charpy impact tests were carried out on unnotched specimens using Zwick 5102 equipment.

All reported data for mechanical tests was computed taking into account the results on five different specimens.

Results and discussion

X-Ray diffraction analyses

Fig. 1a shows the XRD diffractions for the nanocomposites with OMMT and SEBS. As can be seen, the nanocomposite patterns show a sharp peak of low intensity at 2θ of around 2.5° for the
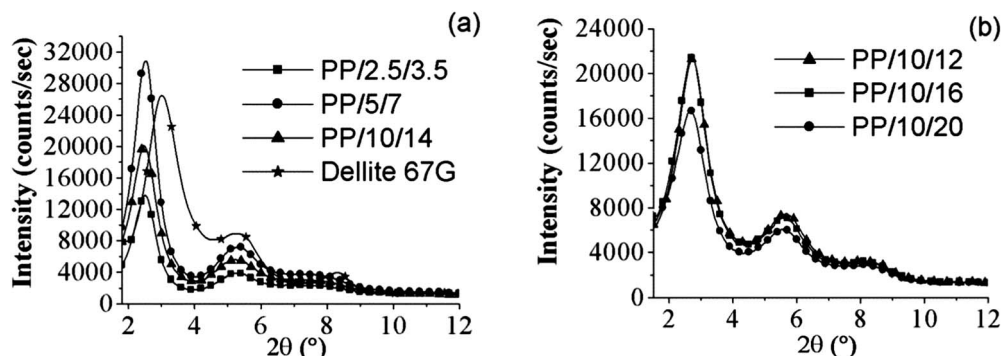
Fig. 1 Nanocomposites X-ray diffractions with (a) different concentration of OMMT (2.5%, 5% and 10%) and SEBS : OMMT ratio 1.4 : 1 and (b) different content of SEBS (12%, 16% and 20%) and 10% OMMT.

2.5 and 10 wt% content of OMMT. These reflections corresponded to an increase of basal distance up to d_{001} of 4.1 nm.

Taking into account that the OMMT initial basal distance was 3.4 nm and that the intensity of the peak decreased, but still remained sharp, it appeared that nanocomposites consisted of an intercalated ordered structure.

When a higher amount of SEBS was added (Fig. 1b) in the nanocomposites with a constant amount of clay of 10 wt%, the nanocomposites presented a broader peak at 2θ of 2.5° with decreased intensity in case of the nanocomposite with 20 wt% load of SEBS. Moreover, inside this peak, two other peaks could be extrapolated which corresponded to a basal distance of 4.4 and 3.7 nm, respectively (Table 2). In this case, the nanocomposites still presented an intercalated structure, but with a higher degree of disorder, confirmed also by the higher values obtained for the half-maximum breadth, $\beta_{1/2}$: β_{001}, β_{002}, β_{003}. However, the peaks at 2θ around 5.3° and 8.35° show that there were stacks of silicate layers which were not exfoliated, probably due to the high amount of block copolymer used, which intercalated between the layers of the silicate by styrene blocks[43] and the elastomers blocks remained outside[21] and probably covered the stacks and blocked them from exfoliating when further processed (Scheme 1).

Crystallization and melting behaviour

The melting temperature increased in nanocomposites with a low concentration of OMMT and SEBS from 166 to 169 °C (Fig. 2a).
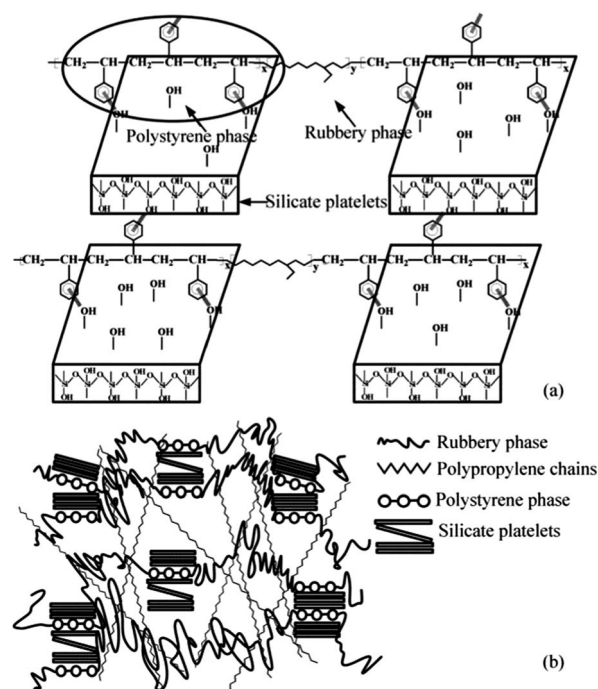
Scheme 1 Schematic representation of possible interaction between materials (a) styrene silicate interaction and (b) interactions within composite structure.

Table 2 Silicate basal distance in PP/SEBS nanocomposites computed from XRD

Sample	$d_{001}{}^{a}$ (Å)	$I_{001}{}^{b}$	$\beta_{001}{}^{c}$ (°)	$d_{002}{}^{a}$ (Å)	$I_{002}{}^{b}$	$\beta_{002}{}^{c}$ (°)	$d_{003}{}^{a}$ (Å)	$I_{003}{}^{b}$	$\beta_{003}{}^{c}$ (°)
Dellite 67G	33.9	6580	1.26	18.92	2316	1.28	—	—	—
PP/2.5/3.5	41.3	2524	1.01	19.47	817	1.64	13.75	770	3.22
PP/5/7	40.9	5734	1.00	19.38	1738	1.70	13.63	1259	3.02
PP/10/12	44.1, 37.3	310, 3777	0.92, 1.20	18.1	1048	1.41	12.2	217	1.38
PP/10/14	40.0	2559	0.99	19.6	631	1.55	13.20	127	1.89
PP/10/16	43.3, 37.2	541, 3431	1.05, 1.16	18.2	954	1.37	12.3	240	1.44
PP/10/20	44.1, 37.6	484, 2384	1.02, 1.13	18.3	840	1.45	12.3	192	1.42

[a] Measured distance between silicate layers. [b] Integrated peak intensity. [c] Full width at half maximum.
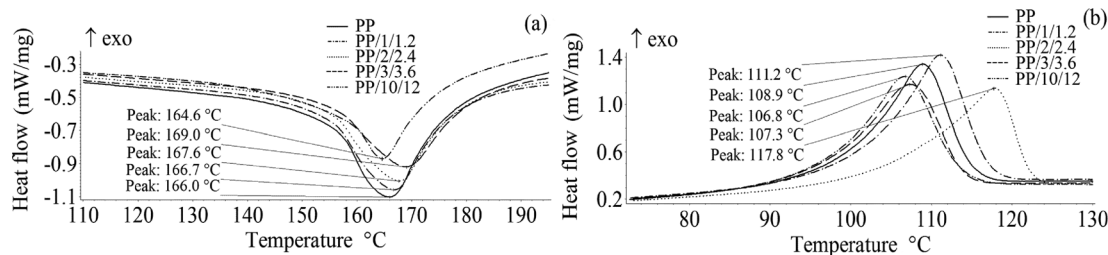
Fig. 2 DSC heating scans of PP and nanocomposites (a) heating scans and (b) cooling scans.

In the case of nanocomposite with a high amount of clay and thus with a high amount of SEBS, the melting temperature decreased to 164.6 °C. Therefore, a high amount of SEBS made the melting temperature to decrease. However, the addition of clay increased the melting temperature and thus, compensated the decrease in melting temperature caused by the increased amount of SEBS.

The cooling exotherms showed an interesting effect (Fig. 2b). The nanocomposites with low amount of clay presented lower crystallisation temperature than polypropylene, which seemed to decrease as the concentration of silicate increased. But, in the nanocomposite with 10 wt% OMMT and 12 wt% SEBS the crystallisation temperature increased up to 117.8 °C, meaning that the formation of crystallites occurred at a higher temperature.[27]

This may be correlated with XRD results which showed that, in the nanocomposites with a high amount of SEBS, the nanocomposites presented a higher disorder structure.

The degree of the crystalline phase was computed from DSC curves at the first run (Table 3). The degree of the crystalline phase of PP increased in nanocomposites.

However, if we compare the samples, the degree of the crystalline phase of PP decreased with the increasing of the SEBS content. Moreover, a high amount of OMMT tends to compensate the decreasing in the crystalline phase induced by a high content of SEBS.

Nanocomposites presented an improved thermostability as compared to the PP matrix (Fig. 3).

The decomposition temperature increased with the amount of the silicate. Although the residue at 550 °C increased, the higher amount was recorded for the nanocomposite with 3 wt% OMMT loading instead of for the one with 10 wt% OMMT loading as it would have been expected. In this latest case, the 4% residue represented the pure silicate (MMT), meaning that

Table 3 Degree of crystallinity for nanocomposites

Sample name	Crystalline phase[a] (%)
PP	46.9
PP/10/12	50.5
PP/10/16	48.4
PP/10/20	49.1

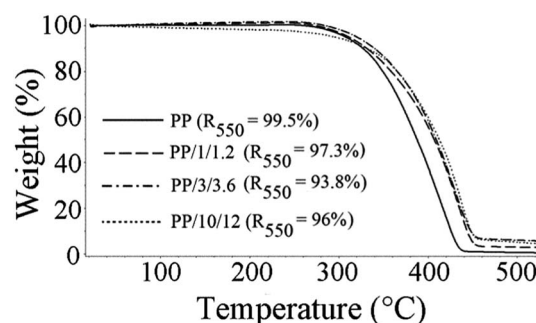[a] Degree of crystallinity from DSC measurements.

Fig. 3 Thermostability of nanocomposites.

all the organic phase decomposed. As was observed from XRD, the nanocomposites with a lower amount of OMMT present an ordered intercalated structure, which may be the reason of an increased residue in the nanocomposite with 3 wt% OMMT; an ordered structure of clay platelets may block the gases to diffuse while decomposition occurs.

Transition electron microscopy

Clay particles were rather well dispersed in the polymeric matrix (Fig. 4). However, no full exfoliation was obtained. In this case,
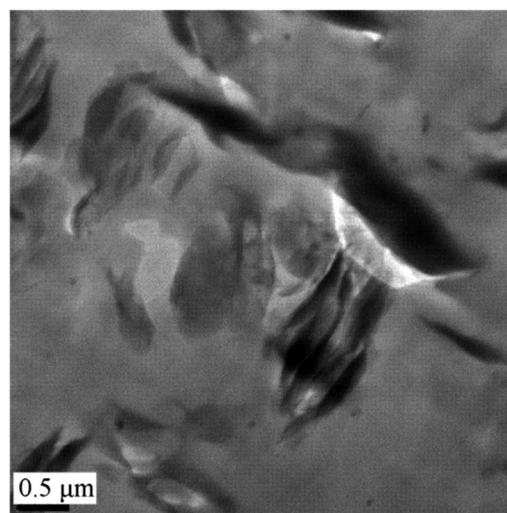

Fig. 4 Bright field-TEM image of PP/10/12 at scale 0.5 μm.

the nanocomposite still presented an intercalated structure, but with a higher degree of disorder, confirmed also by X-ray diffractions.

A TEM image of PP/10/12 shows that there were stacks of silicate layers which were still agglomerated. This sustained the XRD observations, that when a higher amount of block copolymer was used, this intercalated between the silicate layers and the excess covered and blocked the stacks from exfoliating when further processed.

Mechanical properties

Tensile properties. Mechanical results presented the variation of mechanical properties as function of composition (Table 4).

Considering the binary compositions it can be observed that using SEBS caused a reduction in the tensile strength and Young's modulus, but the impact strength increased if compared to neat PP. Moreover, a significant increase was observed from 2.2 to 41.7 kJ m^{-2} when a concentration of 30 wt% SEBS was used.

These results are in accordance with previous reports found in literature which show that an elastomer can improve impact strength of neat PP, but with the sacrifice of tensile strength.[44,45] On the other hand, using OMMT presents a decrease in the tensile strength and unmodified impact strength, while the Young's modulus increases.[46]

Nanocomposites presented an increased stiffness and impact strength, and a small decrease in tensile strength. It can be noticed that the impact strength increased with the amount of SEBS, while the tensile strength decreased with it. The decrease of tensile strength was below the value of neat PP. Young's modulus of nanocomposites decreased with the increase of SEBS concentration. Although Young's modulus decreased, the values were not below neat PP values; this decrease was overcome by the addition of OMMT.

The dispersion at nanometer scale of OMMT/SEBS concentrate into the PP matrix formed intercalated structures, which corresponded to the formation of a percolated nanostructure in nanocomposites. As shown in previous reports,[40,47,48] mechanical properties of neat PP can be improved by this percolated nanostructure. Moreover, the clay platelets orientation may also contribute to the reinforcement effects.

The influence of SEBS concentration in nanocomposites is presented in Fig. 5. It can be observed that toughness increased with the increase of SEBS concentration while stiffness decreased. Although the stiffness decreased, it still remains higher than that of the neat PP.

Impact strength. Unnotched Charpy and notched Izod impact tests were performed on nanocomposites (Fig. 6). Both tests are in accordance and present the same behaviour of the nanocomposites.

A significant improvement of 64% in Charpy impact strength can be noticed for the nanocomposites with 10 wt% OMMT and 12 wt% SEBS. Furthermore, when Izod impact strength was tested for the nanocomposite with 10 wt% OMMT and 14 wt% SEBS, the increase was spectacular, of 300% as compared with neat PP. To the authors' best knowledge, until now, such a high improvement of impact strength has not been reported for PP nanocomposites reinforced with OMMT/SEBS filler.
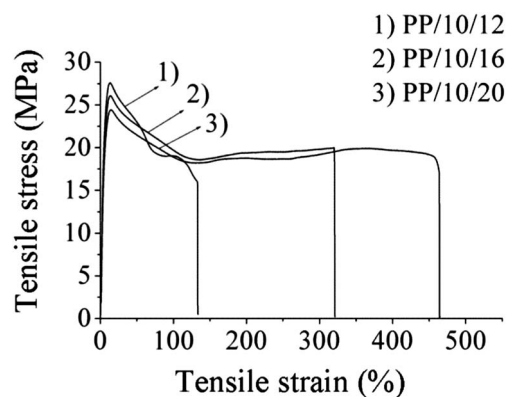

Fig. 5 Stress–strain curves for SEBS high loading nanocomposites.

Table 4 Mechanical properties for obtained nanocomposites

| Sample	Tensile stress at break (MPa)	Tensile stress at yield (MPa)	Axial strain at break (%)	Young's modulus of elasticity (MPa)	Energy at break (J)	Izod impact strength, (kJ m^{-2})
PP	17.9 ± 1.7	37.2 ± 3.3	88.5 ± 17.6	771 ± 53	43.3 ± 11.7	2.2 ± 0.3
PP/0/13.5	16.5 ± 0.8	27.3 ± 0.8	256 ± 14.8	608 ± 146	92.2 ± 8.8	19.3 ± 0.1
PP/0/18.4	17.5 ± 0.6	25.1 ± 0.6	358 ± 57.1	539 ± 167	118.7 ± 23.3	17.6 ± 0.5
PP/0/23	15.6 ± 0.1	24.1 ± 1.2	286 ± 48.5	478 ± 121	98.1 ± 15.5	33.3 ± 0.2
PP/0/30	22.4 ± 1.2	20.2 ± 0.1	583 ± 42	427 ± 24	187 ± 13.6	41.7 ± 0.8
PP/5/0	27.9 ± 0.3	33.3 ± 0.3	35.1 ± 1.3	757 ± 56	18.7 ± 1.4	2.1 ± 0.1
PP/12/0	26.2 ± 0.2	30.6 ± 0.2	34.1 ± 7.2	830 ± 53	17.6 ± 3.8	2.0 ± 0.3
PP/13/0	25.8 ± 0.4	30.6 ± 0.4	26.0 ± 3.6	831 ± 44	13.0 ± 2.4	1.9 ± 0.1
PP/2.5/3.5	16.0 ± 7.0	29.7 ± 0.9	112.7 ± 37.5	1715 ± 158	37.6 ± 25.1	3.3 ± 0.2
PP/5/7	19.8 ± 2.8	27.2 ± 0.3	199.0 ± 18.2	1297 ± 99	99.2 ± 11.8	5.0 ± 0.9
PP/10/12	15.5 ± 0.4	27.7 ± 0.1	114.7 ± 19	1045 ± 96	42.5 ± 8	7.6 ± 0.4
PP/10/14	12.7 ± 1.1	21.5 ± 0.4	181.6 ± 11.8	1012 ± 37	74.5 ± 2.1	8.9 ± 0.1
PP/10/16	18.2 ± 0.5	26.3 ± 0.2	301.3 ± 90	936 ± 48	105.8 ± 40	20.3 ± 2.5
PP/10/20	16.8 ± 0.3	24.1 ± 0.3	420.5 ± 41	954 ± 38	138.9 ± 33	34.6 ± 0.5
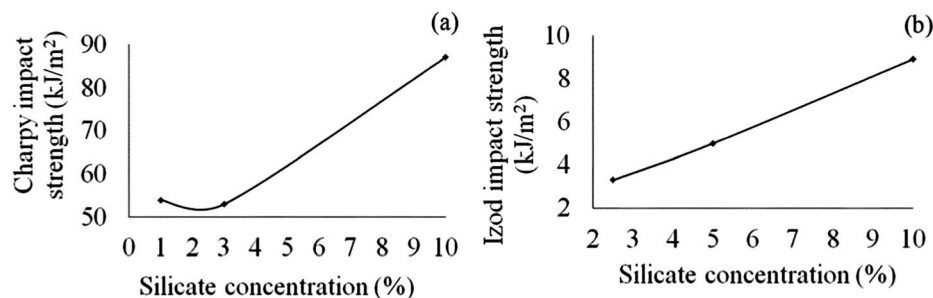
Fig. 6 Impact strength (a) unnotched Charpy impact strength and (b) notched Izod impact strength.

Creep and cyclic loading. In addition to the static tensile tests, creep and cyclic measurements were carried out in order to evaluate the failure resistance and dimensional stability of the nanocomposites compared to the neat PP.

The creep performance of the neat PP and the nanocomposites were characterized by the creep strain as a function of creep time under a constant stress. The creep test results of different OMMT/SEBS loadings are presented in Fig. 7.

Nanocomposites were subjected for one hour to an applied stress of 21 MPa, which represents 70% of static UTS (ultimate tensile strength) of the neat PP at room temperature. The creep curves presented primary and secondary creep stages. The creep resistance of nanocomposite with 1 wt% was better than that of the neat PP and the nanocomposites with a high level of OMMT content. In fact the creep resistance started to be influenced by the SEBS content from nanocomposites after it reached the value of 3 wt%. However, the creep results were in accordance with static tensile measurements, if the instantaneous elasticity that can be given by the intercept of the creep curve with the strain axes is considered. The shape of the curve presented increase elasticity, thus, increased toughness for the nanocomposites with a higher amount of SEBS than for neat PP.

Cyclic measurements were performed on a high loading consisting of 100 cycles and a variation of stress between 10 and 20 MPa. During the test, samples did not present failure. The results were in accordance with creep measurement results.

In Fig. 8 it can be observed that the nanocomposite with 1 wt% OMMT presented a decrease of strain after 100 cycles, thus an improvement of resistance to failure; whereas for the nanocomposites with a higher amount of OMMT the strain increased. The same phenomenon happened as in resistance to
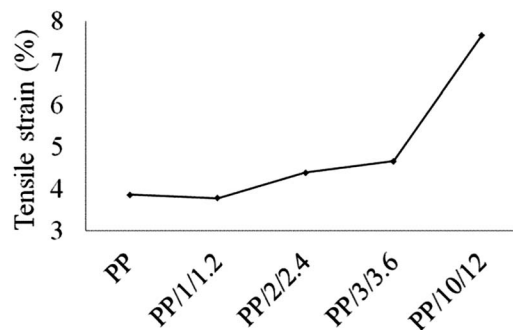

Fig. 8 Strain deformation after 100 cycles.

creep, where the increased amount of SEBS take over and influenced these properties.

Conclusions

Polypropylene nanocomposites were obtained by melt incorporation of an elastomer/OMMT hybrid. X-ray diffraction showed that intercalated nanocomposites were obtained when using SEBS as compatibilizer.

The mechanical properties were correlated with nanocomposites morphologies emphasized by X-ray diffraction. The morphological and mechanical results showed that the components strongly influenced the properties of the nanocomposites. Taking into consideration the ratio between the compatibilizing agent/organosilicate, nanocomposites with either toughness or stiffness or with good balance between toughness–stiffness properties can be obtained. Moreover nanocomposites presented a spectacular improvement of impact strength. Therefore, considering the overall properties, these types of nanocomposites can easily find applications in the automotive industry.

Acknowledgements

References

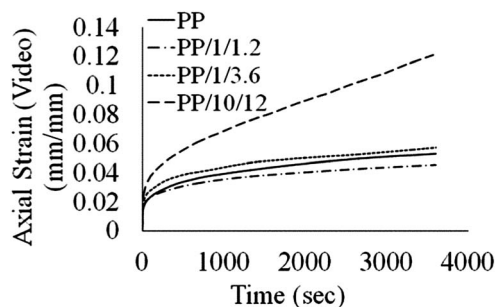1 Z. Martin, I. Jimenez, M. A. Gomez, H. Ade and D. A. Kilcoyne, *Macromolecules*, 2010, **43**, 448.

Fig. 7 Creep resistance in time of nanocomposites.

2 R. A. Vaia, K. D. Jandt, E. J. Kramer and E. P. Giannelis, *Macromolecules*, 1995, **28**, 8080.

3 S. S. Ray and M. Okamoto, *Prog. Polym. Sci.*, 2003, **28**, 1539.

4 F. Mammeri, E. LeBourhis, L. Rozesa and C. Sanchez, *J. Mater. Chem.*, 2005, **15**, 3787.

5 K. Kalaitzidou, H. Fukushima and H. Miyagawa, *Polym. Eng. Sci.*, 2007, **47**, 1796.

6 C. G. Sanporean, Z. Vuluga, J. d. Christiansen, C. Radovici, E. A. Jensen and H. Paven, *Ind. Eng. Chem. Res.*, 2013, **52**, 3773.

7 N. Stribeck, A. Zeinolebadi, M. G. Sari, S. Botta, K. Jankova, S. Hvilsted, A. Drozdov, R. Klitkou, C. G. Potarniche, J. d. Christiansen and V. Ermini, *Macromolecules*, 2012, **45**, 962.

8 W. Zhu, C. H. Lu, F. C. Chang and S. W. Kuo, *RSC Adv.*, 2012, **2**, 6295.

9 M. Modesti, A. Lorenzetti, D. Bon and S. Besco, *Polym. Degrad. Stab.*, 2006, **91**, 672.

10 M. Modesti, A. Lorenzetti, D. Bon and S. Besco, *Polymer*, 2005, **46**, 10237.

11 P. Maiti, P. H. Nam and M. Okamoto, *Macromolecules*, 2002, **35**, 2042.

12 D. Garcia-Lopez, O. Picazo, J. C. Merino and J. M. Pastor, *Eur. Polym. J.*, 2003, **39**, 945.

13 S. Hambir, N. Bulakh and J. P. Jog, *Polym. Eng. Sci.*, 2002, **42**, 1800.

14 J. Li, M. T. Ton-That and S. J. Tsai, *Polym. Eng. Sci.*, 2006, **46**, 1060.

15 Z. Martin, I. Jimenez, M. A. Gomez, H. W. Ade, D. A. Kilcoyne and D. Hernadez-Cruz, *J. Phys. Chem. B*, 2009, **113**, 11160.

16 S. P. Lonkar, A. Leuteritza and G. Heinrich, *RSC Adv.*, 2013, **3**, 1495.

17 M. Ardanuy, J. I. Velasco, M. Antunes, M. A. Rodriguez-Perez and J. A. de Saja, *Polym. Compos.*, 2010, **31**, 870.

18 M. Ranjbar, A. Arefazar and G. H. Bakhshandeh, *Advanced Research in Physics and Engineering 2nd WSEAS Int. Conf. on Nanotechnology*, 2010, p. 113.

19 S. C. Tjong, S. P. Bao and G. D. Liang, *J. Polym. Sci., Part B: Polym. Phys.*, 2005, **43**, 3112.

20 S. C. Tjong and S. P. Bao, *Compos. Sci. Technol.*, 2007, **67**, 314.

21 S. P. Bao and S. C. Tjong, *Composites, Part A*, 2007, **38**, 378.

22 D. J. Carastan and N. R. Demarquette, *Macromol. Symp.*, 2006, **233**, 152.

23 C. H. Lee, H. B. Kim, S. T. Lim, H. S. Kim, Y. K. Kwon and H. J. Choi, *Macromol. Chem. Phys.*, 2006, **207**, 444.

24 W. Xia, P. Shao-Long, Y. Jun-He and Y. Fan, *Trans. Nonferrous Met. Soc. China*, 2006, **16**, 524.

25 B. Ohlsson, H. Hassander and B. Tornell, *Polym. Eng. Sci.*, 1996, **36**, 501.

26 B. Ohlsson and B. Tornell, *Polym. Eng. Sci.*, 1996, **36**, 1547.

27 H. L. Chen, L. Y. Zhou, Q. Ye and J. Chen, *Mod. Plast. Process. Appl.*, 2004, **16**, 42.

28 A. Phillips, P. W. Zhu and G. Edward, *Polymer*, 2010, **51**, 1599.

29 M. Kato, A. Usuki and A. Okada, *J. Appl. Polym. Sci.*, 1997, **66**, 1781.

30 C. M. Chan, J. Wu, J. X. Li and Y. K. Cheung, *Polymer*, 2002, **43**, 2981.

31 S. C. Tjong, S. A. Xu, R. K. Y. Li and Y. W. Mai, *J. Appl. Polym. Sci.*, 2003, **87**, 441.

32 S. C. Tjong, S. A. Xu, R. K. Y. Li and Y. W. Mai, *J. Appl. Polym. Sci.*, 2002, **86**, 1303.

33 J. E. Stamhuis, *Polym. Compos.*, 1984, **5**, 202.

34 S. C. Tjong, S. A. Xu, R. K. Y. Li and Y. W. Mai, *Compos. Sci. Technol.*, 2002, **62**, 831.

35 M.-K. Seo and S.-J. Park, *Chem. Phys. Lett.*, 2004, **395**, 44.

36 K. L. Edwards, *Mater. Des.*, 2004, **25**, 529.

37 J. M. Garces, D. J. Moll, J. Bicerano, R. Fibiger and D. G. McLeod, *Adv. Mater.*, 2000, **23**, 1835.

38 P. Elisek and M. Raab, *Engineering Against Fracture*, proceedings of the 1st conference, Springer, 2009, p. 81, ISBN 978-1-4020-9401-9.

39 S. M. Lloyd and L. B. Lave, *Environ. Sci. Technol.*, 2003, **37**, 3458.

40 F. H. Su and H. X. Huang, *J. Appl. Polym. Sci.*, 2009, **112**, 3016.

41 Z. Vuluga, D. M. Panaitescu, C. Radovici, C. Nicolae and M. D. Iorga, *Polym. Bull.*, 2012, **69**, 1073.

42 S. B. Roy, B. Ramaraj, S. C. Shit and S. K. Nayak, *J. Appl. Polym. Sci.*, 2011, **120**, 3078.

43 Y. L. Li and L. Zhao, *ACS Appl. Mater. Interfaces*, 2011, **3**, 1613.

44 J. Yin, Y. Zhang and Y. X. Zhang, *J. Appl. Polym. Sci.*, 2005, **98**, 957.

45 S. Wu, *J. Appl. Polym. Sci.*, 1988, **35**, 549.

46 M. Jerabek, Z. Major, K. Renner, J. Moczo, B. Pukanszky and R. W. Lang, *Polymer*, 2010, **51**, 2040.

47 C. G. Ma, Y. L. Mai, M. Z. Rong, W. H. Ruan and M. Q. Zhang, *Compos. Sci. Technol.*, 2007, **67**, 2997.

48 C. Ding, D. M. Jia, H. He, B. C. Guo and H. Q. Hong, *Polym. Test.*, 2005, **24**, 94.